Published in final edited form as:
Gene Expr Patterns. 2010 ; 10(7-8): 361–367. doi:10.1016/j.gep.2010.08.004.

Expression patterns of astrocyte elevated gene-1 (AEG-1) during development of the mouse embryo

Hyun Yong Jeon[a], **Murim Choi**[d], **Eric L. Howlett**[a,b], **Nikollaq Vozhilla**[a], **Byoung Kwon Yoo**[a], **Joyce A. Lloyd**[a], **Devanand Sarkar**[a,b,c], **Seok-Geun Lee**[e,*], and **Paul B. Fisher**[a,b,c,*]

[a]Department of Human and Molecular Genetics, Virginia Commonwealth University School of Medicine, Richmond, VA 23298

[b]VCU Massey Cancer Center, Virginia Commonwealth University School of Medicine, Richmond, VA 23298

[c]VCU Institute of Molecular Medicine, Virginia Commonwealth University School of Medicine, Richmond, VA 23298

[d]Department of Genetics, The Howard Hughes Medical Institute, Yale University School of Medicine, New Haven, CT 06510

[e]Cancer Preventive Material Development Research Center, College of Oriental Medicine, Kyung Hee University, Seoul 130-701, Republic of Korea

Abstract

Expression of astrocyte elevated gene-1 (AEG-1) is elevated in multiple human cancers including brain tumors, neuroblastomas, melanomas, breast cancers, non-small cell lung cancers, liver cancers, prostate cancers, and esophageal cancers. This gene plays crucial roles in tumor cell growth, invasion, angiogenesis and progression to metastasis. In addition, over-expression of AEG-1 protects primary and transformed cells from apoptosis-inducing signals by activating PI3K-Akt signaling pathways. These results suggest that AEG-1 is intimately involved in tumorigenesis and may serve as a potential therapeutic target for various human cancers. However, the normal physiological functions of AEG-1 require clarification. We presently analyzed the expression pattern of AEG-1 during mouse development. AEG-1 was expressed in mid-to-hindbrain, fronto-nasal processes, limbs, and pharyngeal arches in the early developmental period from E8.5 to E9.5. In addition, at stages of E12.5-E18.5 AEG-1 was localized in the brain, and olfactory and skeletal systems suggesting a role in neurogenesis, as well as in skin, including hair follicles, and in the liver, which are organ sites in which AEG-1 has been implicated in tumor development and progression. AEG-1 co-localized with Ki-67, indicating a role in cell proliferation, as previously revealed in tumorigenesis. Taken together, these results suggest that AEG-1 may play a prominent role during normal mouse development in the context of cell proliferation as well as differentiation, and that temporal regulation of AEG-1 expression may be required during specific stages and in specific tissues during development.

*To whom correspondence should be addressed: Dr. Paul B. Fisher, Professor and Chair, Department of Human and Molecular Genetics, Director, VCU Institute of Molecular Medicine, Virginia Commonwealth University School of Medicine, Sanger Hall 11-015, 1101 East Marshall Street, Richmond, VA 23298, Phone: 1-804-828-9632; Fax: 1-804-827-1124, pbfisher@vcu.edu and Seok-Geun Lee seokgeun@khu.ac.kr.

Keywords

AEG-1; development; mouse embryo; cell proliferation; cancer

1. Results and Discussion

Astrocyte elevated gene-1 (AEG-1) was originally cloned by our group as a human immunodeficiency virus-1 (HIV-1)- and tumor necrosis factor (TNF)-α-inducible gene in primary human fetal astrocytes (PHFA) using a Rapid Subtraction Hybridization (RaSH) approach (Jiang et al., 2000; Su et al., 2002; Su et al., 2003; Kang et al., 2005). Although the role of AEG-1 induction in astrocyte function or HIV-1-associated dementia has not been elucidated, recent studies revealed that the expression of *AEG-1* is significantly implicated in tumor progression, metastasis of tumors and overall patient survival in many human cancers including brain tumors, neuroblastoma, hepatocellular carcinoma (HCC), breast cancer, non-small cell lung cancer (NSCLC), esophageal squamous cell carcinoma (ESCC), and prostate cancer (Brown et al., 2004; Kikuno et al., 2007; Yoo et al., 2009; Song et al., 2009; Yu et al., 2009; Lee et al., 2009; Hu et al., 2009; Emdad et al., 2010). These studies also showed that aberrant expression of AEG-1 modulated cancer progression by activating multiple signaling pathways, including PI3K-Akt, ERK, p38MAPK and the nuclear factor (NF)-κB pathways (Emdad et al., 2006; Emdad et al., 2007; Kikuno et al., 2007; Sarkar et al., 2008; Yoo et al., 2009; Song et al., 2009; Yu et al., 2009; Lee et al., 2009; Emdad et al., 2009; Emdad et al., 2010). In addition, AEG-1 itself is a downstream target of oncogenic Ras and mediates the growth promoting effects of Ras, and also activates cell survival pathways through the PI3K-Akt pathway (Lee et al., 2006; Lee et al., 2008). Recent observations also demonstrate that AEG-1 can induce oncogenic transformation as well as angiogenesis (Emdad et al., 2009). The mouse *AEG*-1 gene was cloned by *in vivo* phage screening as Metadherin, a gene mediating metastasis of breast cancer cells to the lung (Brown et al., 2004). Taken together, these findings indicate that *AEG*-1 may play a fundamental and global role in cancer development and progression.

The functional attributes of AEG-1 have been explored in tumor development and progression using xenograft models or established cell lines. Transgenic mouse models, which will permit analysis of the *in vivo* functions of AEG-1 in normal physiology and cancer development and progression, are not currently available. In the present study, we examined the expression pattern of AEG-1 in mouse embryonic tissues in which progenitor cells exist for differentiation and cell proliferation for tissue and organ formation, in order to provide initial insights into the potential physiological roles of AEG-1 in normal development.

1.1. Expression and localization of AEG-1 in mouse embryos at E8.5, E9.5 and E10.5

When a vaginal plug was found in the morning, this was considered E0.5. For the initial assessment of *AEG*-1 expression pattern during early developmental stages, mRNAs were extracted from the whole wild-type mouse embryos at E8.5, E9.5 and E10.5 and subjected to quantitative real-time PCR. *AEG*-1 mRNA was detected in varying degrees from these three stages, with peak expression at E10.5 (Fig. 1A). To further address the spatial and temporal expression pattern of AEG-1, whole mount immunohistochemistry was performed on E9.5 and E10.5 embryos. As shown in Figure 1B, AEG-1 was expressed throughout the dorsal midline and extending cranially to the fronto-nasal process at E9.5. In addition, forelimb, hindlimb and pharyngeal arches were strongly immunostained. At E10.5, a similar expression pattern persisted in these organs, most notably in the mid-to-hindbrain, fronto-nasal process, limbs, and anterior pharyngeal arches (Fig. 1B).

With the onset of neurogenesis, neuroepithelial cells differentiate into radial glial cells and basal progenitor cells, and most of the neurons in the brain are derived from these cells. In mice, this transition occurs throughout most of the brain between E10 and E12 (Götz et al., 2005). In addition, the first pharyngeal arches (PA) subdivide into maxillary and mandibular portions, which give rise to the palate and jaw, respectively (Lievre, 1974; Noden, 1983). The second PA is differentiated into the otic pit, which develops into the inner ear (Streit, 2001). Another important embryological structure, the fronto-nasal process, generates the olfactory system in which neurogenesis begins to occur at E10 (Murdoch et al., 2007). Based on these results and the robust expression of in the early developmental stages we hypothesize that AEG-1 expression plays a pertinent role in progenitor cell differentiation and/or proliferation of early embryos.

1.2. Expression of AEG-1 in the developing brain

AEG-1 expression was notable in the developing brain region (Fig. 1B), suggesting a role during early stages of brain morphogenesis. Embryos were collected from E10.5 to E18.5 and mRNA was prepared from the developing brain. Consistent with the whole-mount data, there was relatively strong expression of *AEG*-1 in the brain at E10.5 compared to later stages of mouse development (Fig. 2A), but its expression was greatly decreased by E18.5 (Fig. 2A). As shown in Fig. 2B, AEG-1 was mainly detected in the neuroectoderm and cephalic mesenchyme at E10.5, when the brain tube is developed through formation of a neuropore from E9.5 (Bard et al., 1998). The AEG-1 expression pattern of the developing brain during E12.5-18.5 was also analyzed by immunohistochemistry on the paraffin sections. In the cerebrum and cortex, AEG-1 was most evident at E12.5, was detectable at E14.5, and was not detectable at E16.5 and E18.5 (Fig. 2C). In addition, lateral ventricle is filled with cerebrospinal fluid to protect and nourish both the brain and spinal cord. The cerebrospinal fluid is secreted by choroid plexus (CP) within the lateral ventricle and derives some components from exchange across the cerebral endothelial cells (Dziegielewska et al., 2001). Unlike the cerebrum and cortex, the CP showed consistent AEG-1 staining throughout all of the observed stages (Fig. 2C).

1.3. Expression of AEG-1 in the spinal cord and olfactory system

To examine the relationship between AEG-1 expression and neurogenesis, we next focused on the developing spinal cord and olfactory system, in addition to the brain, where neuronal development is well documented (Hatten, 1999). At E12.5, segmenting cartilage primordium of vertebra is beginning to be formed along the vertebral axis (Fig. 3A). However, there was no distinct AEG-1 expression at E12.5 in this region. Interestingly, a strong signal was observed from cartilage primordium of the spinal column and in the root ganglia at E14.5 (Fig. 3A). At E16.5 and E18.5, the degree of expression is apparently diminished, albeit maintaining a similar expression pattern (Fig. 3A). Together with the results in the developing brain, these findings suggest that AEG-1 could be important in the development of neural tube that comprises the brain and spinal cord. In addition, AEG-1 was weakly stained in the nucleus pulposus (NP) in the middle of the spinal disc at E18.5, but not in the annulus fibrosus (AF) surrounding the nucleus pulposus (Fig. 3A). There are two distinct cell types, chondrocyte-like cells and notochordal cells, that mainly reside in the NP located in the intervertebral disk. NP is required for the generation and maintenance of the disk structure, and embryonic NP is formed from the embryonic notochord (Setton et al., 2006). Choi et al. (2008) reported that the notochord begins to segregate along the anteroposterior axis at E12.5, and cells of the notochord aggregate in areas where the NPs were forming at E15.5. By E16.5, the cells form the disk-shaped condensation between the vertebrae. Therefore, further studies are required to determine exactly which of the cells in the NP express AEG-1.

Interestingly, AEG-1 expression was also noticeable in the olfactory epithelium (Fig. 3B), which consists of well-characterized neurogenic epithelium and develops at about E14 (Smart, 1971; Kawauchi et al., 2004; Beites et al., 2005). AEG-1 was detected along the olfactory epithelium at E12.5-E14.5, but remained only in the apical layer toward the nasal cavity (Fig. 3B). Although the cellular portion expressing AEG-1 is largely reduced at E18.5, these results indicate that the expression profile including the nasal region from E9.5 to E16.5 overlaps with the period of neurogenesis in the olfactory system. Overall these dynamic expression patterns suggest a relevant role of AEG-1 during neurogenesis in the skeletal and olfactory systems.

1.4. Expression of AEG-1 in the developing skin and hair follicle

The skin is composed of dermis and epidermis, and is responsible for the development of epidermal appendages consisting of the hair follicles, sebaceous glands, mammary glands, teeth and external genitalia (Fuchs et al., 2002). Between E12.5 and 18.5, a change in morphology and thickness in the skin was observed (Fig. 4A). Embryos at E12.5 had a less developed thin layer of early epidermis, while E14.5 to E18.5 embryos had a more stratified and thick layers in both the epidermis and dermis of their skin. AEG-1 was expressed in the epidermis compartment of the skin during all stages of development between E12.5 to E18.5 (Fig. 4A). In particular, at stages E14.5 and E16.5, AEG-1 was robustly expressed in a large portion of the epidermis. However, expression of AEG-1 was apparently diminished thereafter and a reduced signal was evident near the epidermis at E18.5. Compared to the epidermis, the dermis displayed a negligible signal at these developmental stages. Since cell proliferation is very active in this period for embryonic epidermis development (Byrne et al., 2003), these results support the hypothesis that AEG-1 may drive cell proliferation in the developing skin.

Hair follicles as skin appendages begin to develop at E14.5, appear to be in the form of a hair germ cell at E16.5, and are characterized by an inner root sheath and engulfment of dermal papilla within the hair bulb on E18.5 (Owens et al., 2008). Early in development, the epithelium grows down into the dermis and the follicles also require intimate interactions and cellular signaling with the epidermis (Jahoda, 1992; Risek et al., 1992). We focused on the region near the mouth, where many developing hair follicles take shape (Fig. 4B), the number increasing so that by E18.5 the majority of the face is covered by hair follicles. AEG-1 was detected in almost all forming hair follicles at E14.5, but the AEG-1 staining at E16.5 was restricted to a small portion of epidermis near the mouth with some hair follicles that formed later still displaying strong AEG-1 expression (Fig. 4B). At E18.5, expression of AEG-1 at the hair follicles was barely detectable (Fig. 4B). Wnt signaling, which AEG-1 activates via ERK42/44 activation facilitating its role in the pathogenesis of HCC, is fundamental for hair-follicle morphogenesis (DasGupta et al., 1999; Yoo et al., 2009).

1.5. Expression of AEG-1 in the developing liver

We also examined the developing liver between E12.5 and E18.5. As shown in Figure 5, the liver has a well-differentiated and denser architecture compared to other organs at E12.5. In addition, a fissure divides the liver into an upper and a lower lobe. Hepatic and hematopoietic cells are easily distinguishable in the fetal liver, and hepatic cells increase in relative abundance between E12.5 and E18.5 (Fig. 5). Unlike the other organs discussed above, AEG-1 was evenly detected in the hepatic cells of the liver at the developmental stages we examined (Fig. 5). These results suggest that AEG-1 may normally be expressed in actively proliferating cells and tissues like liver that have a strong regenerative ability.

1.6. Expression of AEG-1 in limb development

The expression of AEG-1 in limb buds was first observed at E9.5 (Fig. 1B). Subsequent immunohistochemistry staining was performed on embryos at E13.5, E15.5 and post-natal day 1 (Fig. 6A). Since the developing limb has both apoptotic and proliferating characteristics, we examined whether AEG-1 was associated with cell proliferation events of the limb. All digits were distinguishable, and webbing between all digits was observed at E13.5. AEG-1 expression was apparent only in the hand and foot plates with digits and webbing, while the region displaying apoptotic cell death remained clear without any signal (Fig. 6A). At E15.5 there was no webbing between digits and the tips of the digits were tapered and AEG-1 was not detected at this stage and similarly no AEG-1 expression was observed at postnatal day 1 (Fig. 6A). These results also suggest that AEG-1 expression may be intimately involved in cell proliferation during the developmental period and not apoptotic cell death.

1.7. Co-localization of AEG-1 and Ki-67

To confirm whether AEG-1 is related to cell proliferation in the developing embryo, colocalization of AEG-1 and a cell proliferation marker Ki-67 was examined. As described earlier, the embryonic skin at E14.5 is differentiated into epidermis and dermis and AEG-1 was strongly expressed in the epidermal portion of the skin (Fig. 4A). AEG-1 was notably expressed in the epidermis, including hair follicles as well as dermis, whereas Ki-67 expression was more ubiquitous but weaker in the epidermis (Fig. 6B, upper panel). On a single cell level, colocalization of AEG-1 and Ki-67 was observed (Fig. 6B, lower panel). Taken together, these results indicate that AEG-1 is involved in normal cell proliferation during mouse embryonic development.

1.8. Conclusions

In the present study, we examined the expression pattern of AEG-1 during mouse embryo development from stage E8.5 through E18.5. The expression pattern indicates that AEG-1 may contribute to cell proliferation during the early developmental period, and that its temporal and spatial expression is tightly regulated during fetal development. AEG-1 expression was robustly detected in the developing brain, the neural tube, skin and liver, which correlates with organ sites in which AEG-1 has been implicated in cancer development and progression (Lee et al., 2009; Yoo et al., 2009; Sarkar et al., 2009; Emdad et al., 2010). Although AEG-1 is reduced in normal cells after birth, many recent observations have also demonstrated that aberrant overexpression of AEG-1 is intimately involved in various types of human cancers including brain tumors, neuroblastoma, melanoma, liver cancer, esophageal cancer and breast cancer (reviewed in Sarkar et al., 2009). Based on these results, further detailed studies of AEG-1 function during development as well as in normal physiology are warranted. These investigations will also provide insights into the multiple consequences of AEG-1 expression in tumorigenesis of various tissues where AEG-1 is robustly expressed during normal embryonic development, which has potential to reveal new strategies for cancer therapy by targeting AEG-1 or its downstream-regulated pathways.

2. Experimental procedures

2.1. Animals

C57BL/6NCR mice were time-mated and pregnant females were sacrificed to collect the embryos at different embryonic stages (E8.5-E18.5). Our animal facility artificially provides a 12 h light and 12 h dark cycle. Timing of mating most likely takes place in the dark. The vaginal plugs were found early in the morning. This was considered as the first day of

pregnancy and designated as E0.5. The fetuses were isolated from the uterus and dissected under a microscope. They were fixed in 4% (W/V) paraformaldehyde. The VCU Institutional Animal Care and Use Committee approved this study.

2.2. Extraction of total RNA and Real-Time PCR

Total RNA was extracted using TRIzol reagent (Invitrogen) and cDNA was synthesized by SuperScript III Reverse transcriptase (Invitrogen). Real time PCR was performed using ABI 7900 fast real-time PCR system and TaqMan Gene Expression Assays for mouse AEG-1 (Mm00482588 m1, Applied Biosystems) and β-actin (4352933E, Applied Biosystem) according to the manufacturer's instructions (Applied Biosystems). PCR mixtures were incubated at 50 °C for 2 min and 95 °C for 10 min, then each cDNA was synthesized by two steps at 95 °C for 15 min and 60 °C for 1 min during 40 cycles.

2.3. Immunohistochemistry and Immunostaining on whole mouse embryos

The Embryos from E12.5 to E18.5 were embedded in paraffin and 4-mm sections were prepared. Paraffin sections were deparaffinized in xylene and rehydrated through a graded series of ethanol from absolute ethanol to 80% ethanol and finally washed in PBS. For whole mounting immunostaining, dissected Embryos at E8.5-E10.5 were fixed for 1h at room temperature in 4% (W/V) paraformaldehyde. After rinsing in PBS, endogenous hydrogen peroxidase was quenched with 3% H_2O_2 in PBS for 1h. The sections and whole embryos were incubated with 3% skim milk for 1h and developed by avidin-biotin-peroxidase complexes with DAB substrate solution (Vector Laboratories). The sections and whole mounted embryos were incubated with anti-AEG1 (1:200) antibody (Zymed Laboratories Inc.) overnight at 4°C and treated with anti-rabbit IgG biotinylated secondary antibody for 1h at room temperature after rinsing thoroughly in PBS-T. Following incubation with peroxidase complex reagent for 1h, the immunoreactive signals in sections and whole embryos were detected by DAB substrate (DAKO) and counterstained briefly with hematoxylin (Zymed Laboratories Inc.). The sections were then dehydrated, mounted and photographed.

2.4. Immunofluorescence

The sagittal sections of embryos were deparaffinized and permeabilized with 0.1% Triton X-100 in PBS for 30 min. Sections were then blocked for 1h at room temperature with 2% goat serum in PBS and incubated with anti-AEG1 (1:500) (Zymed Laboratories Inc.) and anti-Ki67 (1:1,000) (Cell Signaling Technology) antibodies overnight at 4°C. Sections were then rinsed in PBS and incubated with Alexa Fluor 488–conjugated anti-mouse and Alexa Fluor 546-conjugated anti-rabbit IgG (Molecular Probes; Invitrogen) for 1h at room temperature. The sections were mounted in VECTASHIELD Fluorescence Mounting Medium containing DAPI (Vector Laboratories). Images were analyzed with a Zeiss 510 Meta confocal imaging system.

Acknowledgments

The present study was supported in part by National Institutes of Health grants R01 CA134721, R01 CA097318 and R01 NS31492, and the Samuel Waxman Cancer Research Foundation to P.B.F., by the Korea Science and Engineering Foundation (KOSEF) grant funded by the Korea government (MEST) (No. 2009-0063466) to S.G.L. and grants from the Goldhirsh Foundation for Brain Tumor Research and the Dana Foundation to D.S. D.S. is the Harrison Endowed Scholar in the VCU Massey Cancer Center. P.B.F. holds the Thelma Newmeyer Corman Endowed Chair in Cancer Research at the VCU Massey Cancer Center and is a Samuel Waxman Cancer Research Foundation Investigator.

References

Bard JBL, Kaufman MH, Dubreuil C, Brune RM, Burger A, Baldock RA, Davidson DR. An internet-accessible database of mouse developmental anatomy based on a systematic nomenclature. Mech Dev. 1998; 74:111–120. [PubMed: 9651497]

Byrne C, Hardman M, Nield K. Covering the limb – formation of the integument. J Anat. 2003; 202:113–124. [PubMed: 12587926]

Brown DM, Ruoslahti E. Metadherin, a cell surface protein in breast tumors that mediate lung metastasis. Cancer Cell. 2004; 5:365–374. [PubMed: 15093543]

Choi KS, Cohn MJ, Harfe BD. Identification of nucleus pulposus precursor cells and notochordal remnants in the mouse: implications for disk degeneration and chordoma formation. Dev Dyn. 2008; 237:3953–3958. [PubMed: 19035356]

DasGupta R, Fuchs E. Multiple roles for activated LEF/TCF transcription complexes during hair follicle development and differentiation. Development. 1999; 126:4557–4568. [PubMed: 10498690]

Dziegielewska KM, Ek J, Habgood MD, Saunders NR. Development of the choroid plexus. Microsc Res Tec. 2001; 52:5–20.

Emdad L, Sarkar D, Lee SG, Su ZZ, Yoo BK, Dash R, Yacoub A, Fuller CE, Shah K, Dent P, Bruce JN, Fisher PB. Astrocyte elevated gene-1 (AEG-1): a novel target for human glioma therapy. Mol Cancer Ther. 2010; 9:79–88. [PubMed: 20053777]

Emdad L, Lee SG, Su ZZ, Jeon HY, Boukerche H, Sarkar D, Fisher PB. Astrocyte elevated gene-1 (AEG-1) functions as an oncogene and regulates angiogenesis. Proc Natl Acad Sci USA. 2009; 106:21300–21305. [PubMed: 19940250]

Emdad L, Sarkar D, Su ZZ, Randolph A, Boukerche H, Valerie K, Fisher PB. Activation of the nuclear factor kappaB pathway by astrocyte elevated gene-1: implications for tumor progression and metastasis. Cancer Res. 2006; 66:1509–1516. [PubMed: 16452207]

Emdad L, Sarkar D, Su ZZ, Lee SG, Kang DC, Bruce JN, Volsky DJ, Fisher PB. Astrocyte elevated gene-1: recent insights into a novel gene involved in tumor progression, metastasis and neurodegeneration. Pharmacol Ther. 2007; 114:155–170. [PubMed: 17397930]

Fuchs E, Raghavan S. Getting under the skin of epidermal morphogenesis. Nat Rev Genet. 2002; 3:199–209. [PubMed: 11972157]

Götz M, Huttner WB. The cell biology of neurogenesis. Nat Rev Mol Cell Biol. 2005; 6:777–788. [PubMed: 16314867]

Hatten ME. Central nervous system neuronal migration. Annu Rev Neurosci. 1999; 22:511–539. [PubMed: 10202547]

Hu G, Chong RA, Yang Q, Wei Y, Blanco MA, Li F, Reiss M, Au JL, Haffty BG, Kang Y. MTDH activation by 8q22 genomic gain promotes chemoresistance and metastasis of poor prognosis breast cancer. Cancer Cell. 2009; 15:9–20. [PubMed: 19111877]

Jiang H, Kang DC, Alexandre D, Fisher PB. RaSH, a rapid subtraction hybridization approach for identifying and cloning differentially expressed genes. Proc Natl Acad Sci USA. 2000; 97:12684–12689. [PubMed: 11058161]

Kang DC, Su ZZ, Sarkar D, Emdad L, Volsky DJ, Fisher PB. Cloning and characterization of HIV-1-inducible astrocyte elevated gene-1, AEG-1. Gene. 2005; 353:8–15. [PubMed: 15927426]

Kawauchi S, Beites CL, Crocker CE, Wu HH, Bonnin A, Murray R, Calof AL. Molecular signals regulating proliferation of stem and progenitor cells in mouse olfactory epithelium. Dev Neurosci. 2004; 26:166–180. [PubMed: 15711058]

Kikuno NH, Shiina, Urakami S, Kawamoto K, Hirata H, Tanaka Y, Place RF, Pookot D, Majid S, Igawa M, Dahiya R. Knockdown of astrocyte-elevated gene-1 inhibits prostate cancer progression through upregulation of FOXO3a activity. Oncogene. 2007; 26:7647–7655. [PubMed: 17563745]

Lee SG, Su ZZ, Emdad L, Sarkar D, Fisher PB. Astrocyte elevated gene-1 (AEG-1) is a target gene of oncogenic Ha-ras requiring phosphatidylinositol 3-kinase and c-Myc. Proc Natl Acad Sci USA. 2006; 103:17390–17395. [PubMed: 17088530]

Lee SG, Su ZZ, Emdad L, Sarkar D, Franke TF, Fisher PB. Astrocyte elevated gene-1 activates cell survival pathways through PI3K-Akt signaling. Oncogene. 2008; 27:1114–1121. [PubMed: 17704808]

Lee SG, Jeon HY, Su ZZ, Richards JE, Vozhilla N, Sarkar D, Van MT, Fisher PB. Astrocyte elevated gene-1 contributes to the pathogenesis of neuroblastoma. Oncogene. 2009; 28:2476–2484. [PubMed: 19448665]

Lievre CL. Role of mesectodermal cells arising from the cephalic neural crest in the formation of the branchial arches and visceral skeleton. J Embryol Exp Morphol. 1974; 31:453–477. [PubMed: 4849659]

Murdoch B, Roskams AJ. Olfactory epithelium progenitors: insights from transgenic mice and in vitro biology. J Mol Histol. 2007; 38:581–599. [PubMed: 17851769]

Noden DM. The role of the neural crest in patterning of avian cranial skeletal, connective, and muscle tissues. Dev Biol. 1983; 96:144–165. [PubMed: 6825950]

Owens P, Han G, Li AG, Wang XJ. The role of Smads in skin development. J Invest Dermatol. 2008; 128:783–790. [PubMed: 18337711]

Risek B, Klier FG, Gilula NB. Multiple gap junction genes are utilized during rat skin and hair development. Development. 1992; 116:639–651. [PubMed: 1289057]

Sarkar D, Park ES, Emdad L, Lee SG, Su ZZ, Fisher PB. Molecular basis of nuclear factor-kappa B activation by astrocyte elevated gene-1. Cancer Res. 2008; 68:1478–1484. [PubMed: 18316612]

Sarkar D, Emdad L, Lee SG, Yoo BK, Su ZZ, Fisher PB. Astrocyte elevated gene-1: far more than just a gene regulated in astrocytes. Cancer Res. 2009; 69:8529–8535. [PubMed: 19903854]

Setton LA, Chen J. Mechanobiology of the intervertebral disc and relevance to disc degeneration. J Bone Joint Surg Am. 2006; 88(Suppl 2):52–57. [PubMed: 16595444]

Smart IH. Location and orientation of mitotic figures in the developing mouse olfactory epithelium. J Anat. 1971; 109:243–251. [PubMed: 5558232]

Song L, Li W, Zhang H, Liao W, Dai T, Yu C, Ding X, Zhang L, Li J. Over-expression of AEG-1 significantly associates with tumor aggressiveness and poor prognosis in human non-small cell lung cancer. J Pathol. 2009; 219:317–326. [PubMed: 19644957]

Streit A. Origin of the vertebrate inner ear: evolution and induction of the otic placode. J Anat. 2001; 199:99–103. [PubMed: 11523832]

Su ZZ, Kang DC, Chen Y, Pekarskaya O, Chao W, Volsky DJ, Fisher PB. Identification and cloning of human astrocyte genes displaying elevated expression after infection with HIV-1 or exposure to HIV-1 envelope glycoprotein by rapid subtraction hybridization, RaSH. Oncogene. 2002; 21:3592–3602. [PubMed: 12032861]

Su ZZ, Chen Y, Kang DC, Chao W, Simm M, Volsky DJ, Fisher PB. Customized rapid subtraction hybridization (RaSH) gene microarrays identify overlapping expression changes in human fetal astrocytes resulting from human immunodeficiency virus-1 infection or tumor necrosis factor-alpha treatment. Gene. 2003; 306:67–78. [PubMed: 12657468]

Yoo BK, Emdad L, Su ZZ, Villanueuva A, Chiang DY, Mukhopadhyay ND, Mills AS, Waxman S, Fisher RA, Llovet JM, Fisher PB, Sarkar D. Astrocyte elevated gene-1 regulates hepatocellular carcinoma development and progression. J Clin Invest. 2009; 119:465–477. [PubMed: 19221438]

Yu C, Chen K, Zheng H, Guo X, Jia W, Li M, Zeng M, Li J, Song L. Overexpression of astrocyte elevated gene-1 (AEG-1) is associated with esophageal squamous cell carcinoma (ESCC) progression and pathogenesis. Carcinogenesis. 2009; 30:894–901. [PubMed: 19304953]

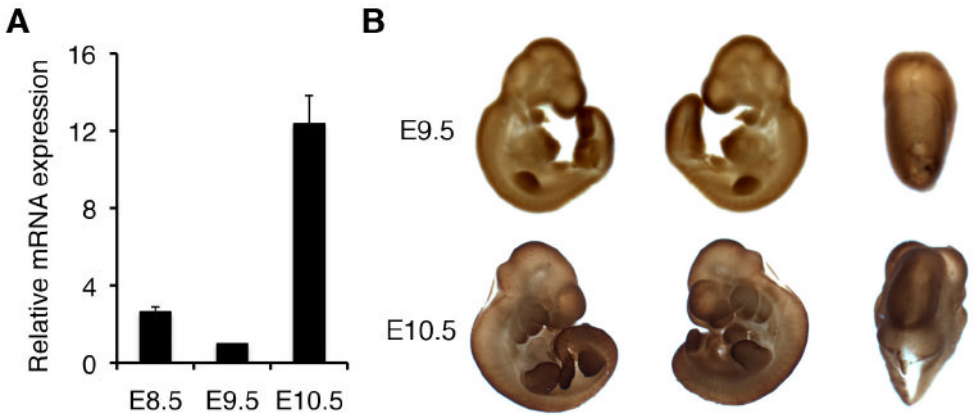

Figure 1. Expression of AEG-1 in the mouse embryo

(A) Real-time PCR at embryonic stages E8.5 to E10.5 and (B) whole mount immunostaining with anti-AEG-1 at E9.5 and E10.5 were performed. Real-time PCR was performed at least three times in duplicate or triplicate, and the minimal number of embryos (n) used at each stage was 9. The expression of *AEG-1* was normalized by *GAPDH*. Error bars indicate SEM.

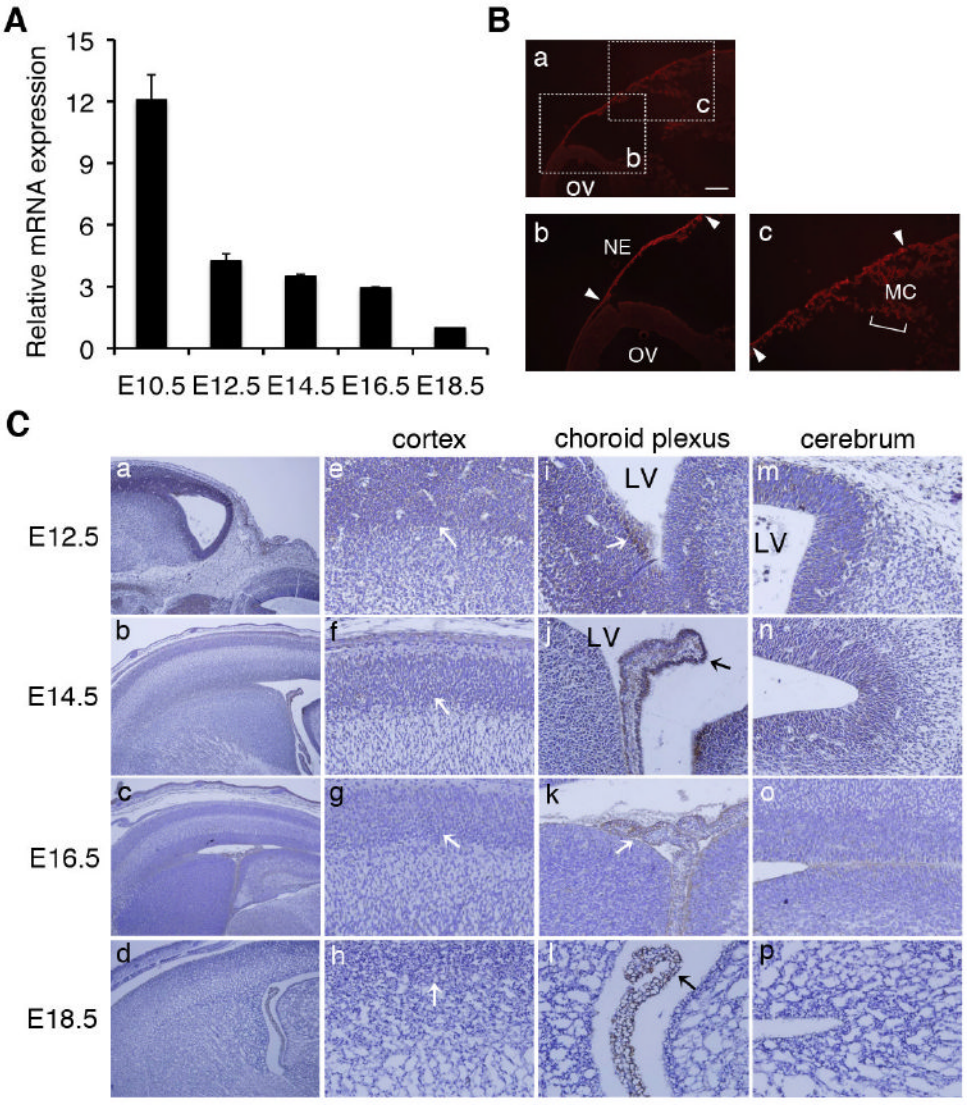

Figure 2. Expression of AEG-1 in the developing brain

(A) Brains were collected from E10.5 to E18.5, and total RNA was prepared. Real-time PCR was performed at least three times in duplicate or triplicate (n=3) and the expression of *AEG-1* was normalized by *GAPDH*. Error bars indicate SEM. (B) The section of the embryonic brain at E10.5 was stained with AEG-1 (Red). The scale bar represents 0.2 mm. OV: optic vesicle, NE: neuroectoderm, and MC: mesenchyme. (C) Immunostaining of brain sections at E12.5 to E18.5 was performed using anti-AEG-1 antibody. The expression of AEG-1 in whole brain (a-d, 100X magnification), cortex (e-h), choroid plexus (i-l) and cerebral region (m-p) (e-p: 200X magnification) were shown. LV: lateral ventricle.

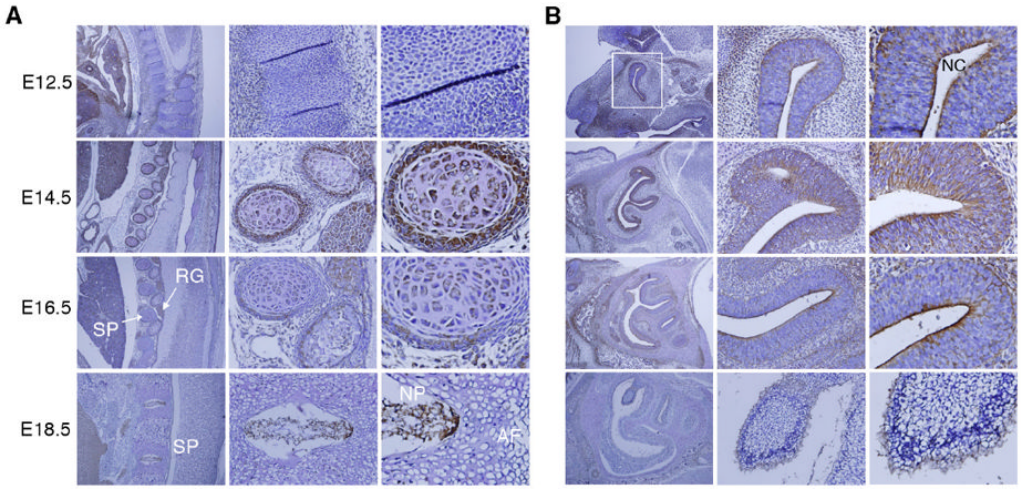

Figure 3. Expression of AEG-1 in the skeletal and olfactory systems

(A) The skeletal system and (B) olfactory system were stained with anti-AEG-1 in E12.5 to E18.5 embryos (*left*, 100X; *middle*, 200X; *right*, 400X). AF: annulus fibrosus, NP: nucleus pulposus, RG: root ganglia and SP: spinal column. White square: Y-shaped olfactory system at E12.5 and NC: nasal cavity.

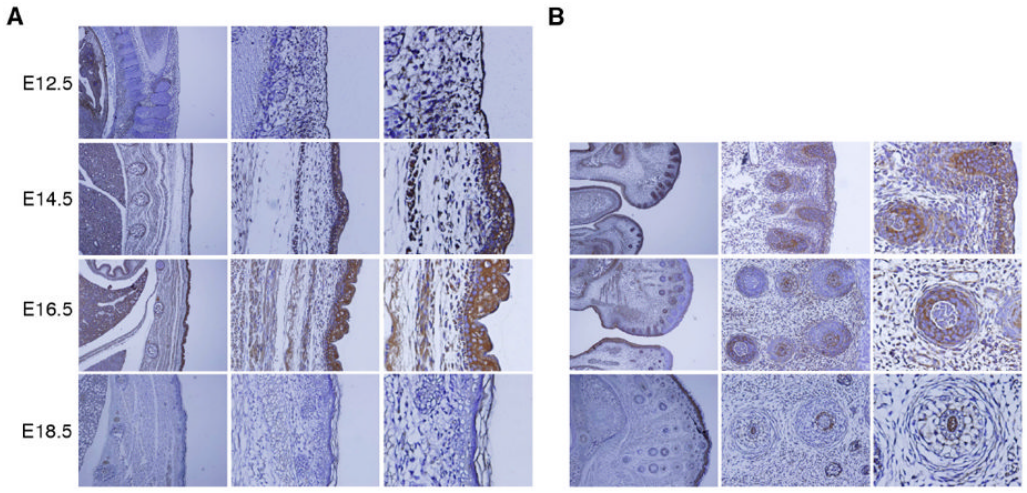

Figure 4. Expression of AEG-1 in the skin and hair follicle

(A) The skin was thin layered at E12.5, and stratified dermis and epidermis were detected at E14.5 to E18.5. Distinct expression of AEG-1 was detected in the epidermis (*left*, 100X; *middle*, 200X; *right*, 400X). (B) AEG-1 was detected in most hair follicles at E14.5, with restricted expression to defined regions at E16.5, and barely detectable at E18.5 (*left*, 100X; *middle*, 200X; *right*, 400X).

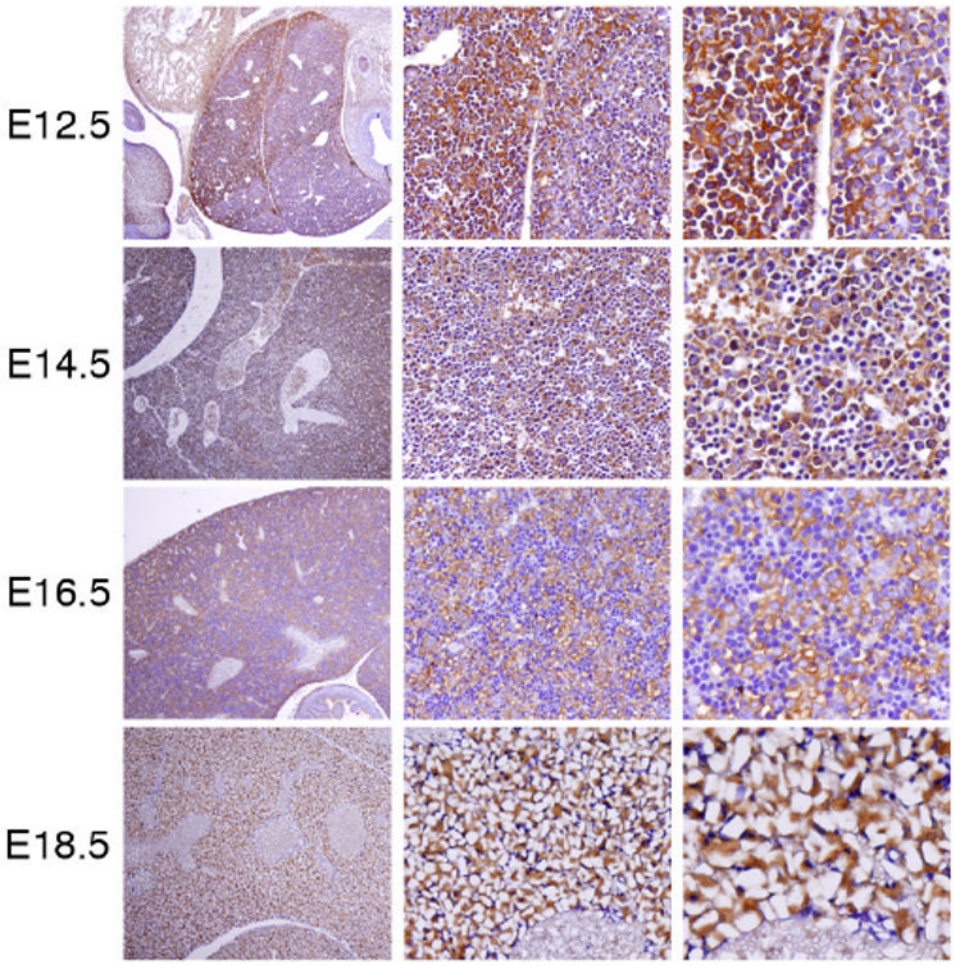

Figure 5. Expression of AEG-1 in the developing liver

Immunohistochemistry was performed on sagittal sections (4 mm) at E12.5 to E18.5. The expression of AEG-1 in liver at each stage is shown (*left*, 100X; *middle*, 200X; *right*, 400X).

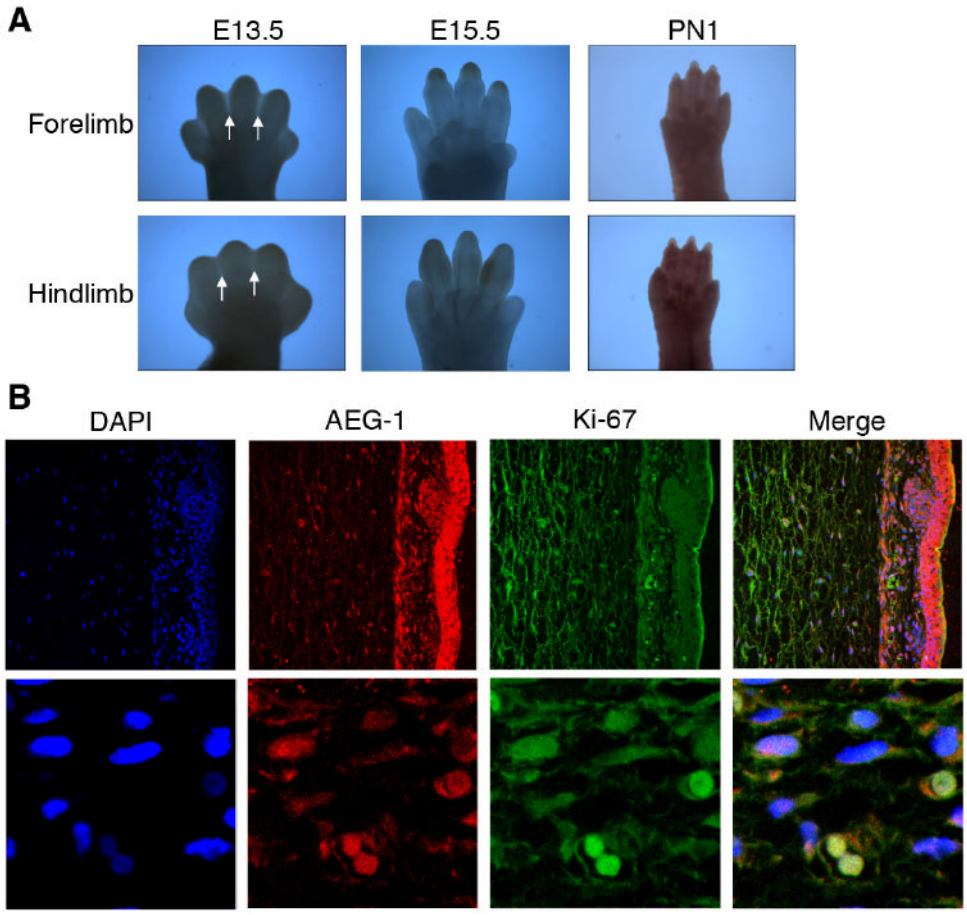

Figure 6. Expression of AEG-1 in the developing limb and its colocalization with Ki-67

(A) The expression of AEG-1 in the limb was examined at E13.5 and E15.5 and at post natal day 1 (D1). (B) The section of the embryonic skin at E14.5 was stained with DAPI (Blue), AEG-1 (Red), and Ki-67 (Green). The parts of dermis and epidermis are shown (*upper panel*, 250X magnification). The cells expressing AEG-1 and Ki-67 in the dermis are magnified (*lower panel*, 1000X).